

Summary Phase II 2015

In the second phase of the project: Experiments on the production of laser ablation jets for HHG and simulations of the transport of radiation in zones E1/E6 and E4/E5, we performed an experimental analysis of the third order harmonic generation (THG) in neon with high intensity laser pulses. We also carried experiments on imaging the ablation plasmas to determine the optimum conditions for high harmonics generation in ablation plumes.

The third order harmonic pulses are produced by focusing near-infrared laser pulses in different types of materials: gases, liquids, solids, laser-generated plasmas, ablated nanoparticles etc. In isotropic (centro-symmetric) media (e.g. gases), for symmetry reasons only odd harmonics are produced, with efficiencies up to 50%. However, the ionization leads to self-induced defocusing of the fundamental laser beam, having a detrimental effect on the HHG process.

Here we present an experimental analysis of third order harmonic generation in neon, determining several laser and gas parameters for the high conversion efficiency, such as: several i.e. focusing parameters-focus length, power laser, gas pressure.

The experimental setup consists of three main parts: the Nd^{3+} :YAG laser operating in the Q-switched regime at $\lambda_p = 1060\text{ nm}$ wavelength, the gas cell containing neon where the third harmonic is generated and the detection system (Fig. 1). Also, we used two filters to select the pump radiation (filter 1, RG 8) and to detect, respectively the third harmonic radiation with $\lambda_3 = 353.3\text{ nm}$ wavelength (filter 2, BG 18).

We used a lens having 10 cm focal length in order to focus the beam into a vacuum cylindrical steel tube having 50 cm length and 3 cm diameter and quartz windows at the edges which is connected to the vacuum pump and the vessel containing neon gas. The pressure in the vacuum system was in the range of 10^{-3} torr, while the pressure of the neon was of about 4.5 torr in order to obtain the maximum conversion efficiency of THG. The gas (neon) is released into the chamber with the aid of a jet nozzle, having a diameter of 5 mm and an adjustable length.

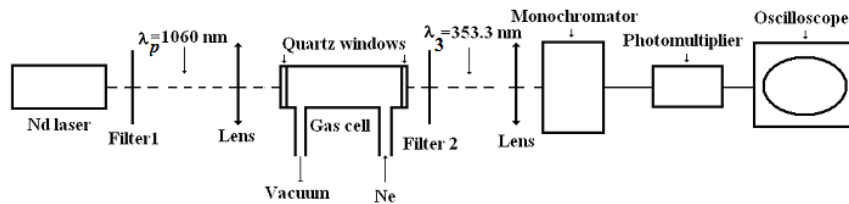


Fig. 1. The experimental setup for THG.

We used a monochromator having 0.03 mm entrance slit, a photomultiplier and an oscilloscope (Tectronix 7613) to detect the harmonic emission (Fig. 2).

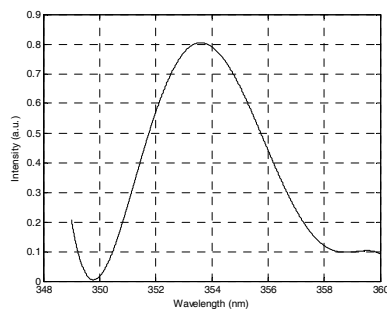


Fig. 2. The spectrum of the third harmonic.

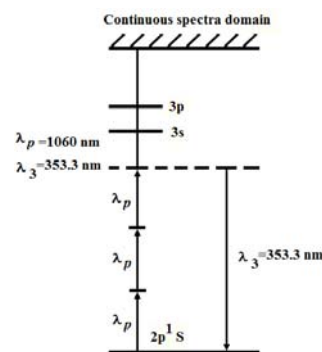


Fig. 3. The scheme of THG.

The neon atoms are excited from the fundamental level, $2p^1s$ by absorption of three photons with $\lambda_p = 1060\text{ nm}$ to a virtual energetic level after that the third harmonic having $\lambda_3 = 353.3\text{ nm}$ wavelength is emitted (Fig. 3).

In the case of 150 kW input pump power of the Nd^{3+} :YAG laser we obtained about 10^{-6} conversion efficiency of the fundamental radiation into the third harmonic radiation which is in good agreement with other experimental results published in the literature.

In typical experiments of high harmonics generation (HHG) in gas jets, harmonics radiation is produced near the laser focus. In the case of a Gaussian laser beam, the phase matching condition, which requires the equality of the vectorial sum of the n fundamental wavevectors to the wavevector of the n th-harmonic, should account for an additional geometric wavevector component (particularly important for the long-wavelength fundamental beam) which arises from the gradient of the Gouy phase. Additional difficulty for efficient HHG is the gas ionization phenomenon which leads to self-defocusing and wave phase mismatch between the harmonics and the fundamental radiation. Experimental and theoretical studies on HHG in gas jets with picosecond and nanosecond laser pulses showed that the right control of the ablation plasma parameters influencing the phase matching conditions leads to efficient HHG if ionization degree smaller than 5% and density is smaller than 10^{19} cm^{-3} . Thus, the characteristics of the gas plume (such as composition, temperature, ionization degree, dimensions) are very important in order to select to low or high harmonics, to increase of the highest harmonic order, and to realize a resonant enhancement of the individual harmonics.

Here we analyzed experimentally the dynamics in ambient air of an ablation gas jet considered as a non-linear medium for HHG by imaging the ablation plasma produced on an Al target. The experimental set-up consists of a „Brilliant” Nd-YAG Q-switched laser system generating 4.5 ns pulses at 1064nm wavelength which are focused at normal incidence on the aluminium target to obtain a spot of ~100 micron diameter and, accordingly, an intensity of ~100 GW/cm². A „Thorlabs” CCD camera with a near field objective and IR 970 nm interferential filter was triggered by the laser system to obtain side images of the ablation plume. Fig. 4 presents the results corresponding to the first three consecutive laser pulses incident on the same area for two irradiation conditions: the target surface is 1 mm behind the focal plane (a-c) and in the focus (d-f), respectively. Figures 4(a) and (d) indicate that the maximum length of the plasma plume produced by the first pulses is ~3 mm while its transversal dimension near the target is ~2mm. Images in Fig. 4(b,c) show that the laser energy is spent in air break-down when the focus is in front of the target. Additionally, the ablation plasma has a non-regular shape in this case as compare to the case where an in focus irradiation geometry is employed (Fig. 4(e,f)).

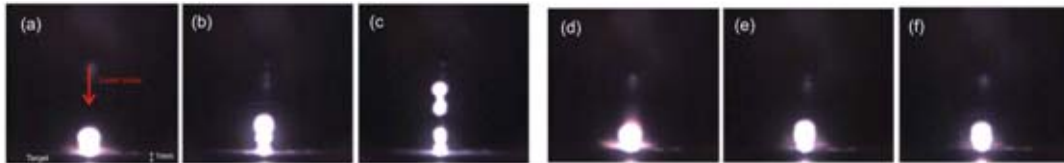


Fig. 4 Ablation plasma images corresponding to the first three consecutive pulses when target is out of focus (a-c) and in focus (d-f)

Also, a realistic modelling of the E1/E6, E4/E5 experimental areas was performed: the dimensions are from the AutoCAD drawing files, the selected materials are complex, as close as possible to those which will be actually used. In Fig. 5 FLUKA and GEANT4 results are presented.

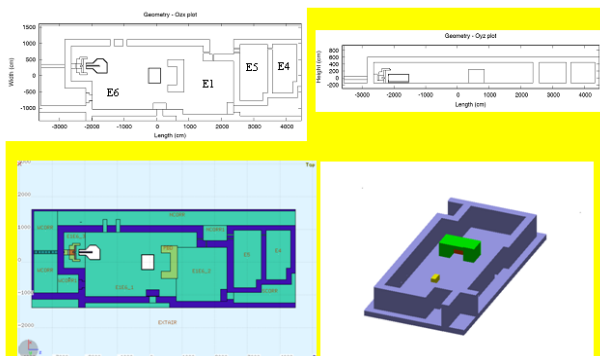


Fig. 5. E1/E6, E4/E5 experimental areas modelled by FLUKA and GEANT4 Monte Carlo transport codes. Above: FLUKA horizontal and vertical projections. Below (right): 3D representation of the GEANT4 geometry.

The GEANT4 geometry file was obtained by following an elaborate procedure, starting from the FLUKA geometry. This involved the following steps: export to OpenSCAD, transformation into *stl* file (with FreeCAD), conversion to the *gdml* format by using InStep (free version). The *gdml* file contains the volumes as tessellated solids made of triangular surfaces. When activating the GDML module, GEANT4 uses the *gdml* files as "in memory" geometry (the material compositions are added manually).

For the heptagonal E6 IC two versions were implemented in FLUKA, one of which included an extension designed to accommodate the relativistic electron spectrometer, also modelled there as a 4 m long permanent magnet with a gap. For each geometry version we calculated the ambient dose equivalent rate corresponding to the electron and proton source terms previously selected.

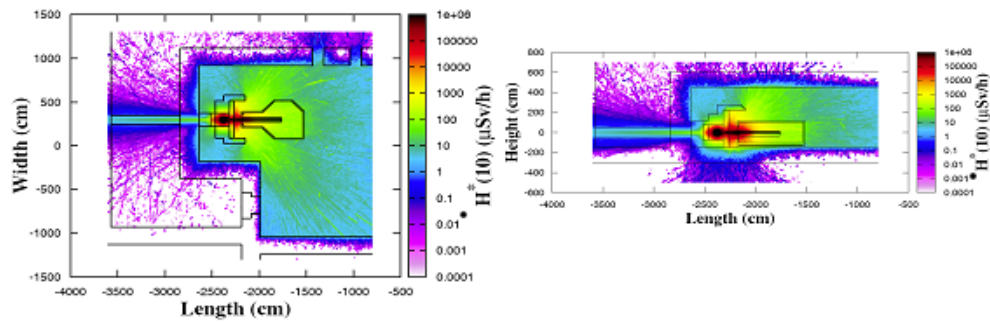


Fig. 6. $H^*(10)$ rate ($\mu\text{Sv/h}$) isodose maps. The 10 cm thick-walled heptagonal IC with an extension and electron spectrometer are represented. The muon shielding (W corridor) behind the W wall and BD can be observed in the in-line direction.

For example, in Fig. 6, 2D isodose map representations of the ambient dose equivalent rate (left - horizontal and right - vertical projections) are presented. The source term is a 38 GeV Gaussian distribution of electrons which could be obtained in a laser acceleration experiment.

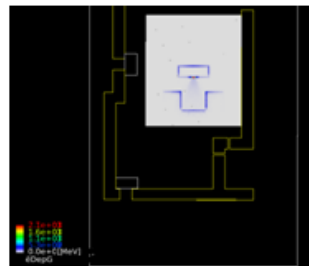


Fig. 7. Absorbed energy per mesh cell (MeV) for secondary photons - SP1 source term.

GEANT4 calculation results of absorbed energy (MeV) due to secondary photons of SP1 (0-100 MeV uniform distribution) are presented in Fig. 7 (5×10^6 protons were generated). Energy contours due to photon absorption in the interaction chamber walls and the frontal regions of the beamdump are observed (the geometry itself is not overlapped on the energy map).

In Fig. 8 (left) a 1D projection gives detailed information on the dose values scored in the in-line direction. Such projections were computed at different positions: floor (in and out - basement), ceiling (in and out - above E6). Finally, the spectra recorded in Fig. 8 (right) show some results of the material study we performed for the muon shielding. We tried soil, ordinary concrete, heavy concrete and iron and the best result was given by iron, especially where high energy muons were concerned. The study should be however supplemented by an activation calculation which will be done in the next stage of this project.

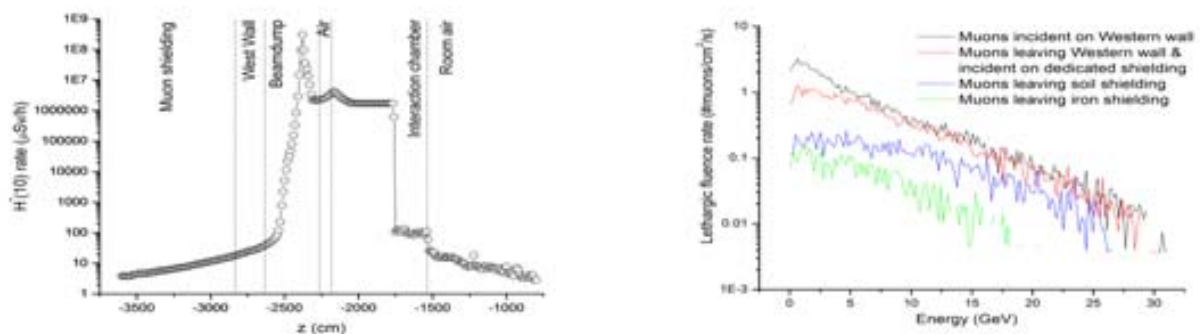


Fig. 8. Left: $H^*(10)$ rate ($\mu\text{Sv/h}$) 1D projection. The scoring was provided in a 10×10 cm xy section column which spans the length of the geometry in the beam line direction (z), at the height of the source (150 cm) above the ground. The main regions crossed by the scoring "column" are presented. Right: Muon spectra for muon shielding design.